International Journal of Thermal Sciences 48 (2009) 2255–2263

Contents lists available at ScienceDirect

International Journal of Thermal Sciences

journal homepage: www.elsevier.com/locate/ijts

Effect of the days scrolling on the natural convection in an open ended storage silo

D.E. Ameziani [a,b], R. Bennacer [b,*], K. Bouhadef [a], A. Azzi [a]

[a] Laboratoire LTPMP, Faculté de Génie Mécanique et Génie des Procédés, USTHB, B.P. 32, 16111 El Allia Bab Ezzouar, Algeria
[b] Université de Cergy Pontoise, L2MGC, 5 mail Gay Lussac 95031, Neuville sur Oise, France

ARTICLE INFO

Article history:
Received 9 October 2008
Received in revised form
31 March 2009
Accepted 13 April 2009
Available online 13 May 2009

Keywords:
Natural convection
Periodical heating
Porous cylinder
Modulation control

ABSTRACT

The problem of unsteady natural convection heat transfer in a vertical, open ended, porous cylinder heated laterally with a sinusoidal time variation of the temperature has been investigated numerically. The model considered is the classical Darcian flow coupled with the energy equation. In the case of constant wall temperature, two types of chimney flows take place, with and without fluid recirculation. The present problem depends on the filtration Rayleigh number (Ra), the aspect ratio (A) and the inlet–outlet conditions (Bi). For low dimensionless temperature amplitudes ($XA < 0.5$) in the sinusoidal time variation, the resulting heat transfer is found to be globally equivalent to the case of constant wall temperature. The observed relative difference between sinusoidal and constant wall temperature is less than 5%. This difference decreases as the Ra is reduced.

1. Introduction

Several devices, such as solar energy collectors, circuits fed by alternating current, storage in ambient conditions, etc., are supplied by a transient input of energy. Therefore, a better knowledge of the mechanisms of heat transfer by transient convection is important. In particular it is of interest to be able to predict the behaviour of a mass of fluid submitted to variable heating conditions, from the existing results obtained with constants imposed temperatures or fluxes.

Many papers are concerned with systems submitted to constant temperatures or fluxes [1–3]. However, such steady situations do not cover, in general, wide cases of industrial and natural situations. Kazmierezak and Chinoda [4] were interested in the transient natural convection in a square cavity, where the hot vertical wall is subjected to a periodical temperature variation. The opposite wall is maintained at a lower constant temperature (cold). They analysed the effects of the period and the oscillating temperature amplitude on the heat transfer through the enclosure. All the obtained transient solutions were found to be periodic in time. It was also demonstrated that the average heat transfer, evaluated for one temporal cycle, was roughly equal to the results obtained for a cavity heated with a constant temperature.

In their experimental work, Mantle-Miller et al. [5] examined transient natural convection for the case where the temperature of the hot bottom wall varied periodically in time around a mean value. The cold upper partition of the cavity is maintained at constant temperature and the vertical walls are adiabatic. For low variations of the temperature amplitude, they showed that the average heat transfer calculated over a cycle was comparable to the permanent heat transfer coefficient obtained from the mean temperature of the hot wall. However, for high temperature modulations, they obtained a difference of more than 10%, between these two considered cases.

Time-dependent heating in porous media has been the subject of relatively few studies, in the past. Sözen and Vafai [6] analysed the behaviour of compressible flows through a packed bed with the inlet temperature or pressure oscillating with time around a non-zero mean value. They found that the oscillation had little effect on the heat storage capacity of the bed. Bradean et al. [7,8] reported analytical and numerical results for flows past a periodically heated or cooled vertical or horizontal plate. They found for the vertical plate, the formation of a row of counter-rotating cells close to the surface. However, when the Rayleigh number is increased above 40, the cellular flow was found to move away from the plate. For the horizontal plate, such a separation effect with Ra did not occur. The effect of the amplitude of the heating of an enclosure was investigated by Antohe and Lage [9]. They showed that the convective flow intensity within the enclosure increases linearly with the heating amplitude.

The aim of the present work is to investigate numerically the problem of unsteady natural convection which occurs in a vertical silo of granular storage, opened at both ends and filled with a saturated porous medium. A varying temperature profile is

* Corresponding author.
E-mail address: bennacer@u-Cergy.fr (R. Bennacer).

1290-0729/$ – see front matter © 2009 Elsevier Masson SAS. All rights reserved.
doi:10.1016/j.ijthermalsci.2009.04.005

Nomenclature

1, 2, 3, 4	considered monitoring times
a	dimensional amplitude
A	aspect ratio, $A = R/H$
$A(i)$	series in Eq. (20)
Bi	Biot number
C_p	heat capacity at constant pressure
$E(m)$	integration coefficient (Eq. (18))
f	regularization function (Eq. (17))
g	gravitational acceleration
h	convective heat exchange coefficient
H	cylinder height
I_n	The nth order Bessel functions
k	thermal conductivity
K	porous media permeability
L	length reference
m	number of terms is the series (Eq. (18))
n	exponential degree of the regularization (Eq. (17))
Nu	Nusselt number
P	dimensionless pressure
Q_T	dimensionless total flow rate
r	dimensionless radial coordinate
R	cylinder radius
Ra	filtration Rayleigh number
Ra_c	critical Rayleigh number
R_k	conductivity ratio, k_{eff}/k_f
t	dimensionless time
T	dimensionless temperature
U	dimensionless longitudinal velocity
V	dimensionless radial velocity
x	dimensionless axial coordinate
XA	dimensionless amplitude

Greek letters

α	thermal diffusivity
β	thermal expansion coefficient
δ	dimensionless boundary layer thickness
λ_m	characteristics values
μ	dynamic viscosity
υ	kinematics viscosity
ρ	fluid density
σ	calorific capacity ratio, $(\rho C_p)_{eff}/(\rho C_p)_f$
τ	dimensionless period

Subscripts

amb	ambient
c	cold
eff	effective
f	fluid
h	hot
m	space averaged value
max	maximum
min	minimum
ref	reference
T	time averaged value

Superscripts

$'$	dimensional variables

imposed on the lateral wall of the enclosure. This condition is applied in order to simulate the scrolling of the days and the years (by changing the period). The study is carried out using the Darcy flow model. The resulting set of governing equations is solved by a finite volumes method.

2. Mathematical formulation

The problem under consideration, namely natural convection in open geometry, is particularly difficult to solve numerically. In fact, the flow rate of the fluid in the channel is imposed indirectly by the intensity of the heated wall. Consequently, most authors do not apply the appropriated boundary conditions for the resolution of the problem. As an illustration of the inaccuracy of the existing approaches, the recently reported benchmark problem of chimney effect was discussed by Desrayaud et al. [10]. The inlet and outlet boundary conditions that have to be applied for this type of problems are complicated by the possible occurrence of reversal flows [11,12].

The physical domain of the flow through the vertical porous cylinder is given in Fig. 1. It is assumed that the flow in the cylinder is axis-symmetric, allowing a two-dimensional approach. The porous medium is considered to be homogeneous, isotropic and saturated with a pure single phase fluid, which is in thermal equilibrium with the solid matrix. The fluid thermo-physical properties are assumed to be constant, except the density in the body force term of the momentum equations where the Boussinesq's approximation is used. The Darcy flow model is assumed to be valid.

The analysis is performed in terms of non-dimensional parameters. To this end, the non-dimensionalization of the governing

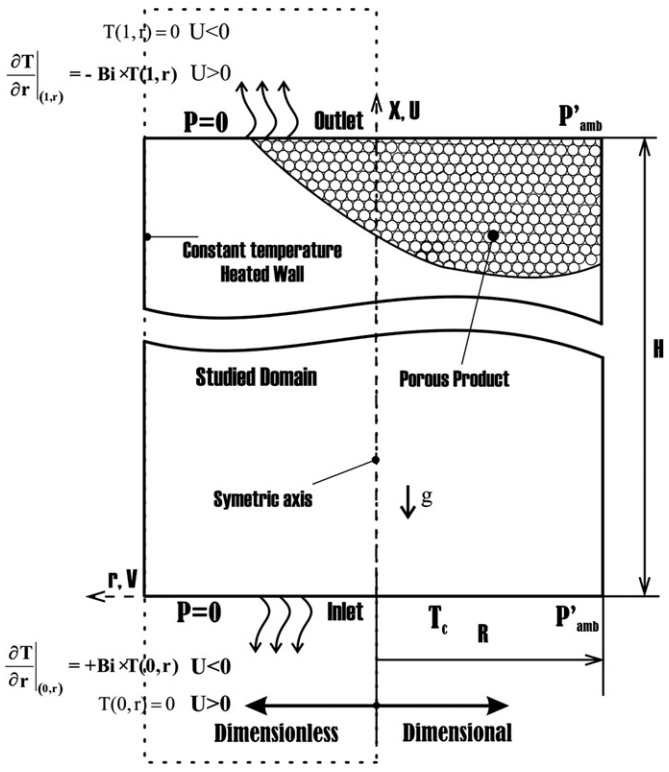

Fig. 1. Geometrical configuration.

equations and boundary conditions is carried out using the following scaling:

$$L_{\mathrm{ref}} = H;\ \Delta T_{\mathrm{ref}} = T'_{\mathrm{h}} - T'_{\mathrm{c}};\ P_{\mathrm{ref}} = \left(\mu\cdot\alpha_{\mathrm{f}}/K\right);$$
$$U_{\mathrm{ref}} = \alpha_{\mathrm{f}}/H \text{ and } t_{\mathrm{ref}} = H^2/\alpha_{\mathrm{f}} \quad (1)$$

The dimensionless quantities are

$$(x,r) = \frac{(x',r')}{L_{\mathrm{ref}}};\ (U,V) = \frac{(U',V')}{U_{\mathrm{ref}}};\ T = \frac{(T'-T'_{\mathrm{c}})}{\Delta T_{\mathrm{ref}}};$$
$$P = \frac{(P'-P'_{\mathrm{amb}})}{P_{\mathrm{ref}}};\ t = \frac{t'}{t_{\mathrm{ref}}} \quad (2)$$

The resulting dimensionless continuity and energy equations are as follows:

$$\frac{\partial^2 P}{\partial x^2} + \frac{1}{r}\frac{\partial}{\partial r}\left(r\frac{\partial P}{\partial r}\right) = Ra\cdot\frac{\partial T}{\partial x} \quad (3)$$

$$\sigma\frac{\partial T}{\partial t} + \left(U\frac{\partial T}{\partial x} + V\frac{\partial T}{\partial r}\right) = R_k\cdot\left(\frac{\partial^2 T}{\partial x^2} + \frac{1}{r}\frac{\partial}{\partial r}\left(r\frac{\partial T}{\partial r}\right)\right) \quad (4)$$

The velocity components are deduced from the obtained pressure field:

$$U = Ra\cdot T - \frac{\partial P}{\partial x};\ V = -\frac{\partial P}{\partial r} \quad (5a,b)$$

where Ra is the filtration Rayleigh number ($Ra = g\beta\Delta T_{\mathrm{ref}}KH/(\nu\cdot\alpha_{\mathrm{f}})$, also called Rayleigh–Darcy number), R_k and σ are respectively the conductivity and calorific capacity ratios (between effective and fluid values).

The dimensionless initial and boundary conditions are then given by

Initially (at $t \le 0$), it is assumed that the pressure and temperature in the cylinder are uniform and equal to those of the ambient conditions:

$$P(x,r,0) = T(x,r,0) = 0 \quad (6)$$

At $t > 0$, the inlet/outlet fluid is supposed to be almost at the ambient pressure, P'_{amb}:

$$P(0,r,t) = P(1,r,t) = 0 \quad (7a,b)$$

Owing to the symmetry requirements at the centre line ($r = 0$) and the impermeable lateral cylinder surface, it follows that:

$$\partial P/\partial r|_{(x,0,t)} = \partial P/\partial r|_{(x,A,t)} = 0 \quad (8a,b)$$

$$\partial T/\partial r|_{(x,0,t)} = 0 \quad (9)$$

Many authors have suggested in the past that the ambient temperature can be approximated by a sum of sinusoidal functions (Boland [13]).

Thus, in the present study, it is assumed that the lateral wall temperature can be described by a sinusoidal time variation (Fig. 2), such that:

$$T(x,A,t) = 1 + XA\cdot\sin((2\pi/\tau)\cdot t) \quad (10)$$

where A is the cylinder aspect ratio $A = R/H$, XA and τ are respectively the dimensionless oscillation amplitude ($XA = a/\Delta T_{\mathrm{ref}}$, where $a = (T_{\max} - T_{\min})/2$), and the period of the sinusoidal variation of the temperature.

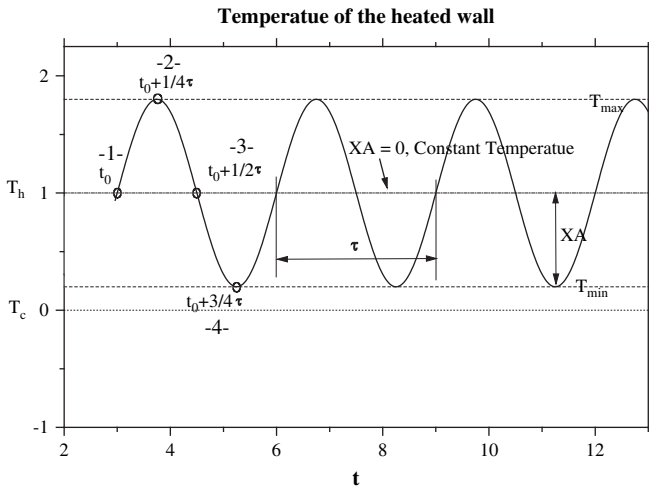

Fig. 2. Time-evolution of the heated wall temperature.

The period can simulate the evolution of the days or that of the years ($\tau_{\mathrm{day}} = \tau_{\mathrm{year}}/365$). On the other hand, the amplitude gives the maximum temperature variation which depends on the geographical situation.

To consider the physical conditions at the bottom and upper surfaces of the enclosure, expressing the interaction between the natural convection through the porous domain and the external ambient fluid, we use the following conditions:

For the top surface:

$$\text{if } U > 0 \text{ (outgoing flow)} \quad \left.\frac{\partial T}{\partial x}\right|_{(1,r,t)} = -Bi\times T(1,r,t) \quad (11a)$$

$$\text{if } U < 0 \text{ (ingoing flow)} \quad T(1,r,t) = 0 \quad (11b)$$

For the bottom surface:

$$\text{if } U > 0 \text{ (ingoingflow)} \quad T(0,r,t) = 0 \quad (12a)$$

$$\text{if } U < 0 \text{ (outgoingflow)} \quad \left.\frac{\partial T}{\partial x}\right|_{(0,r,t)} = +Bi\times T(0,r,t) \quad (12b)$$

where $Bi = h\cdot H/k_{\mathrm{eff}}$ represents the equivalent Biot number of the porous matrix–air interface. h is the convective exchange coefficient and k_{eff} the porous media effective conductivity.

Heat transfer through the system is represented in term of local Nusselt number defined as

$$Nu(x,t) = -\left.\frac{\partial T(x,r,t)}{\partial r}\right|_{r=A} \quad (13)$$

The space averaged Nusselt number along the cylinder is defined as

$$Nu = Nu(t) = \overline{Nu(x,t)} = \int_0^1 Nu(x,t)\cdot \mathrm{d}x \quad (14)$$

and the time averaged total Nusselt number is given by

$$Nu_{\mathrm{T}} = \frac{1}{\tau}\int_0^{\tau} Nu(t)\cdot \mathrm{d}t \quad (15)$$

The resulting transient dimensionless total flow rate (chimney effect) is expressed as

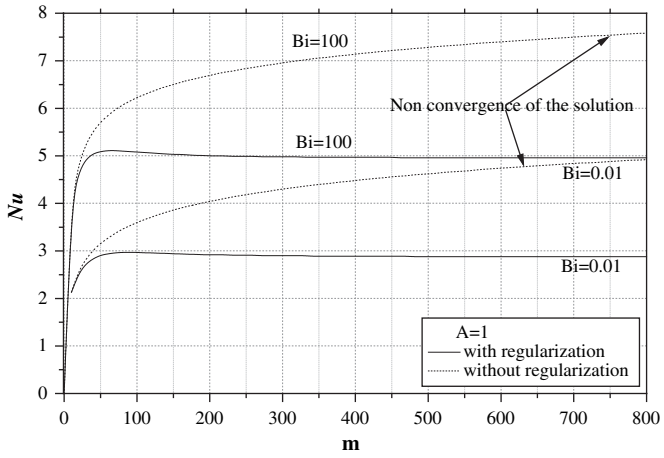

Fig. 3. Effect of the regularization on the analytical solution.

$$Q_T(t) = 2\pi \int_0^A U(1,r,t)\cdot r\cdot dr \tag{16}$$

3. Numerical procedure

The governing equations (Eqs. (3)–(5)) with the associated initial and boundary conditions (Eqs. 6–12) are solved using the finite volumes method, introduced by Spalding (see Patankar [14]), which is based on solving the different equations obtained by integrating the governing equations over control volumes enclosing the nodal points. The resulting algebraic system can be solved by an iterative procedure using the alternate direction implicit method (ADI). An error less than 10^{-6} over all grid points is adopted as the convergence criterion for the pressure and the temperature variables. The results reported in this work are obtained using at least 81×81 irregular grid distribution. For some cases, the threshold convergence value is exceeded and a finer grid must be used. The numerical program is tested for both the pure conduction and the classical Darcy natural convection problem in a square porous cavity.

We underline the existence of singularities at the cylinder wall edges, where the cold and hot surfaces are in direct contact, i.e. the local temperature gradient tends to infinity. In a physical situation, the relaxation phenomenon induces a connection domain in which the temperature decreases from hot to cold values. To reach a grid independence and to converge towards a unique solution, the singularity is treated using temperature regularization on the wall (see for instance Bennacer et al. [15] and Ameziani et al. [16]) as

$$f(x) = T(x,A,t) = \left(1-(1-2\cdot x)^{2n}\right)^2 + XA\cdot\sin((2\pi/\tau)\cdot t) \tag{17}$$

The 'n' value controls the domain affected by the temperature transition. It is found that $n=50$ is enough to reach an asymptotic situation, where no grid effect and only a small domain is affected by the temperature transition (Δx less than 0.001).

In the case of the steady state pure conduction and for a constant applied temperature, an analytical solution is obtained, using variable separation, as

$$T(r,x) = \sum_{m=1}^{m=\infty}[E(m)\cdot I_0(\lambda_m\cdot r)\cdot\sin(\lambda_m\cdot x)] \tag{18}$$

where I_0 is the zero order Bessel function, λ_m is the solutions of the equation $-\lambda_m = Bi\,tg(\lambda_m)$ and $E(m)$ is the integration coefficients taking into account the external applied irregular temperature condition, given by

$$E(m) = \frac{2}{I_0(\lambda_m\cdot A)}\int_0^1\left(1-(1-2\cdot x)^{2n}\right)^2.\sin(\lambda_m\cdot x)\,.dx \tag{19}$$

It is noted that the integral $E_{2n}(m) = (2/I_0(\lambda_m))[-1/\lambda_m(\cos(\lambda_m x)-1) - 2A(2n) + A(4n)]$ is given by a successive integration-by-parts procedure where the coefficients are necessary and have a first series element:

$$A(0) = \frac{1}{\lambda_m}(1-\cos(\lambda_m\cdot x)) \tag{II-20}$$

And a series of

$$A(i) = -\frac{1}{\lambda_m}\left[\frac{1+(-1)^i}{2} + 2i(-1)^i A(i-1)\right] \tag{II-21}$$

Eq. (18), combined with the Nusselt expression (Eqs. (13) and (14)) gives the analytical expression of the resulting heat transfer (averaged Nusselt number) as

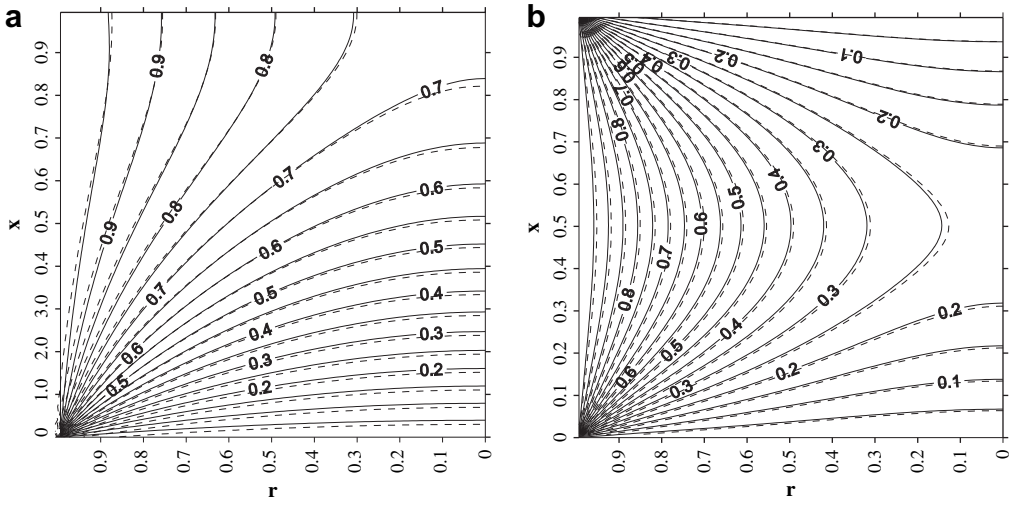

Fig. 4. Analytical and numerical temperature field (a) $Bi \ll 1$ and (b) $Bi \gg 1$.

Table 1
Comparison of Nu_m with some previous numerical results in a confined domain for $A = 1$, $Bi \ll 1$.

Authors	*Ra*	
	10^2	10^3
Walker and Homsy [17]	3.097	12.960
Trevisan and Bejan [18]	3.270	18.380
Lauriat and Prasad [19]	3.090	13.410
Nithiarasu et al. [20–22]	2.970	11.460
Nithiarasu and Ravindran [23]	2.988	12.303
Baytas [24]	3.160	14.060
Massarotti et al. [25]	3.039	13.464
Bennacer et al. [26]	3.110	13.480
Saeid and Pop [27]	3.100	13.442
Present results	3.140	13.580

$$Nu = \sum_{m=1}^{m=\infty} [E(m) \cdot I_1(\lambda_m \cdot A) \cdot (1 - \cos(\lambda_m))] \quad (22)$$

where I_1 is the first order Bessel function.

The obtained series solutions ('m' in Eq. (22)) are represented in Fig. 3. The effect of m on the corresponding Nu with and without ($f(x) = 1$) regularization is compared. We can observe the good convergence of the analytical solution with m in case of regularization. The case with singularities at the corners (without regularization $f(x) = T(x, A) = 1$) leads to an obvious non-convergence of the analytical solution (Eq. (22)). The numerical resolution of this last case exhibits a relative convergence with grids refinement.

The present code is validated, in the conductive regime, by comparing the numerical temperature fields with the analytical one, as illustrated in Fig. 4. The results are obtained for two

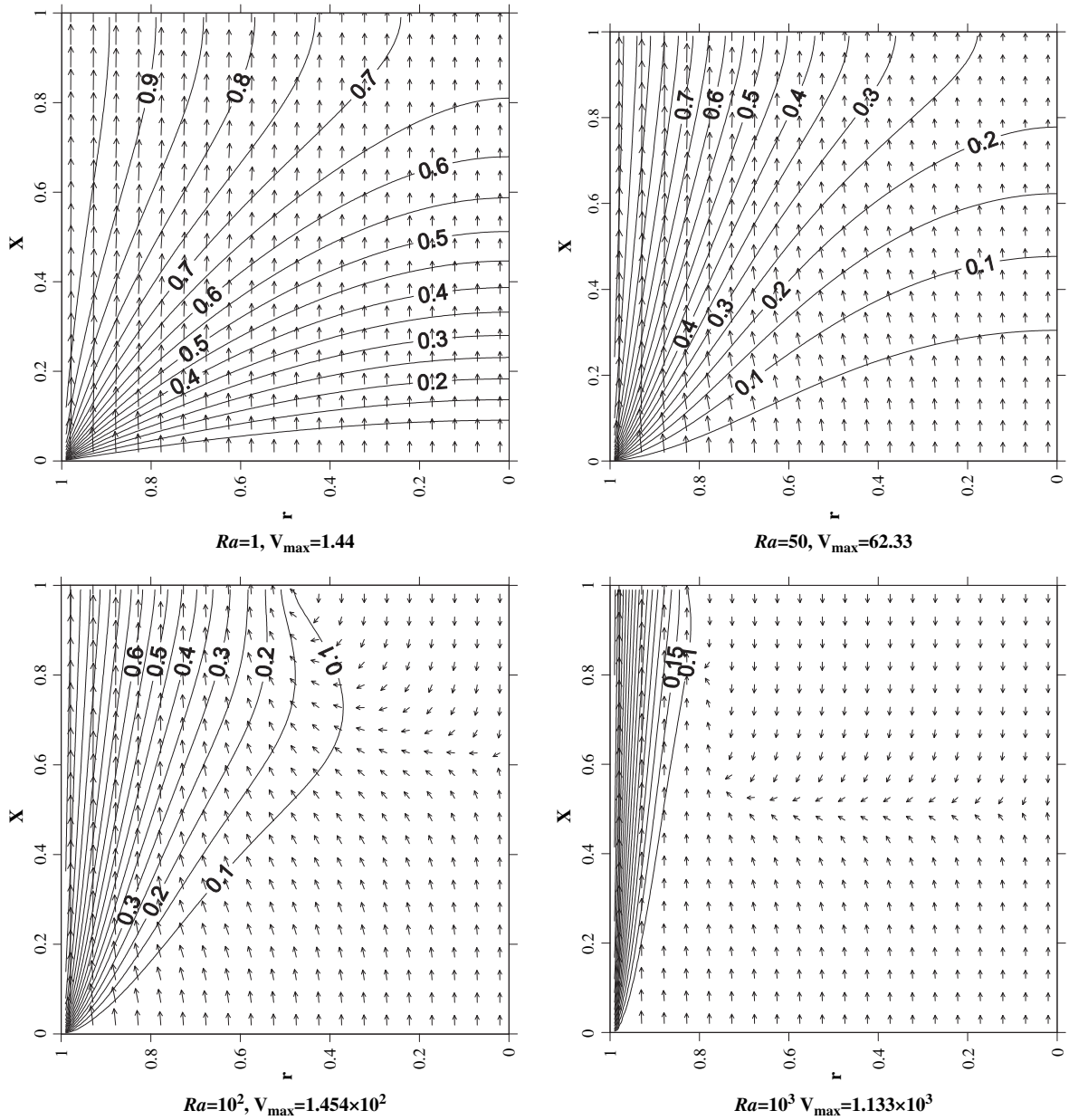

Fig. 5. Temperature and velocity vector fields for different *Ra* ($Bi = 0.01$, $A = 1$, $XA = 0$).

different applied boundary conditions on the horizontal surfaces, namely constant temperatures ($Bi >> 1$) and adiabatic ($Bi << 1$) ones, respectively. The numerical results are represented by solid lines and the analytical solution by the dashed lines (Fig. 4). It is clear from these results that a good agreement is obtained for the different aspect ratio considered. The observed differences in Fig. 4 (right side) are due to our choice to represent the analytical solution by series of $m = 140$ in order to distinguish the numerical–analytical representation. For series of $m > 350$, the analytical and numerical results are in very good agreement

For natural convection, the numerical model is validated adopting the classical Darcy natural convection problem in a square porous cavity. The comparison between our numerical results with previous works, based on the average Nusselt number (Nu_m), is shown in Table 1, for $Ra = 10^2$ and $Ra = 10^3$. A good agreement is also observed in convective regime for the two values of Ra considered.

4. Results

The results are presented and discussed in terms of velocity, pressure and temperature fields. Plots showing the evolution of space and time averaged Nusselt numbers are also presented. Due to the number of variables involved in the present problem, all calculations have been performed for a conductivity ratio, aspect ratio and calorific capacity ratio of unity, i.e. $R_k = A = \sigma = 1$.

4.1. Constant wall temperature

Fig. 5 shows temperature and velocity fields for various Rayleigh numbers in the case of $Bi = 0.01$. The isotherms are similar to those reported for a semi-infinite porous medium bounded by a heated vertical plate. The results indicate that heat propagates from the heated vertical cylinder towards the top of the domain, creating significant thermal gradients in the horizontal/vertical direction. The flow intensity is maximum near the heated wall region and minimum near the centre, where thermal buoyancy forces are weak. The velocity vector field shows that, for small filtration Rayleigh number values ($Ra = 1$ and 50), the flow is ascendant over the entire domain. The resulting, relatively weak flow is mainly unidirectional.

When Ra increases, the thermal boundary layer thickness reduces, generating a reduction of thermal gradients in the core of the porous cylinder. In such situation, the velocity values near the wall increase, and the fluid flow in the cylinder is supplied both from the bottom and partially from the top surface of the domain. This can be explained by the fact that a pressure gradient occurs in the bulk of the cylinder "cylinder centre line" (Fig. 6) without any other buoyancy forces. The resulting volume forces induce a counter-flow in the region around the centre line. This phenomena is a direct consequence of the increase of Ra, for which the thermal boundary layer reaches an adequate scale in comparison with the cylinder radius. The fluid in the cylinder centre is at rest and the two counter-flows indicate the existence of stagnation lines (cf. Fig. 6). Note that this result is in good agreement with that reported by Benasrallah et al. [28], while studying the thermal equilibrium in a porous cylinder subjected to a constant flux. The existence of reverse flows is observed to occur in for a large range of Bi values. The Ra number required to obtain reverse flows dependents strongly on Bi and aspect ratio.

In the case of $A = 1$, Fig. 7 gives the critical Rayleigh number, for the appearance of a top fluid aspiration, for different values of Bi. We can categorize the critical Ra behaviour according to the fact that the Biot number is weak, high or moderate.

The two first behaviours (weak and high values of Bi) correspond to the two extreme asymptotical situations (i.e. thermal field not function of the Biot number values) equivalent to isotherm ($Bi \gg 1$) or adiabatic ($Bi \ll 1$) applied boundary conditions.

The increase of Ra_c with Bi is a direct consequence of the flow intensity (chimney effect) decrease. Such flow intensity decreases are related to the effect of the thermal boundary condition inducing a fluid cooling in the upper cylinder part.

It is noted that the weak and high Bi values exhibit two asymptotic tendency for which the critical Rayleigh numbers are $Ra_c = 52$ and 73, respectively.

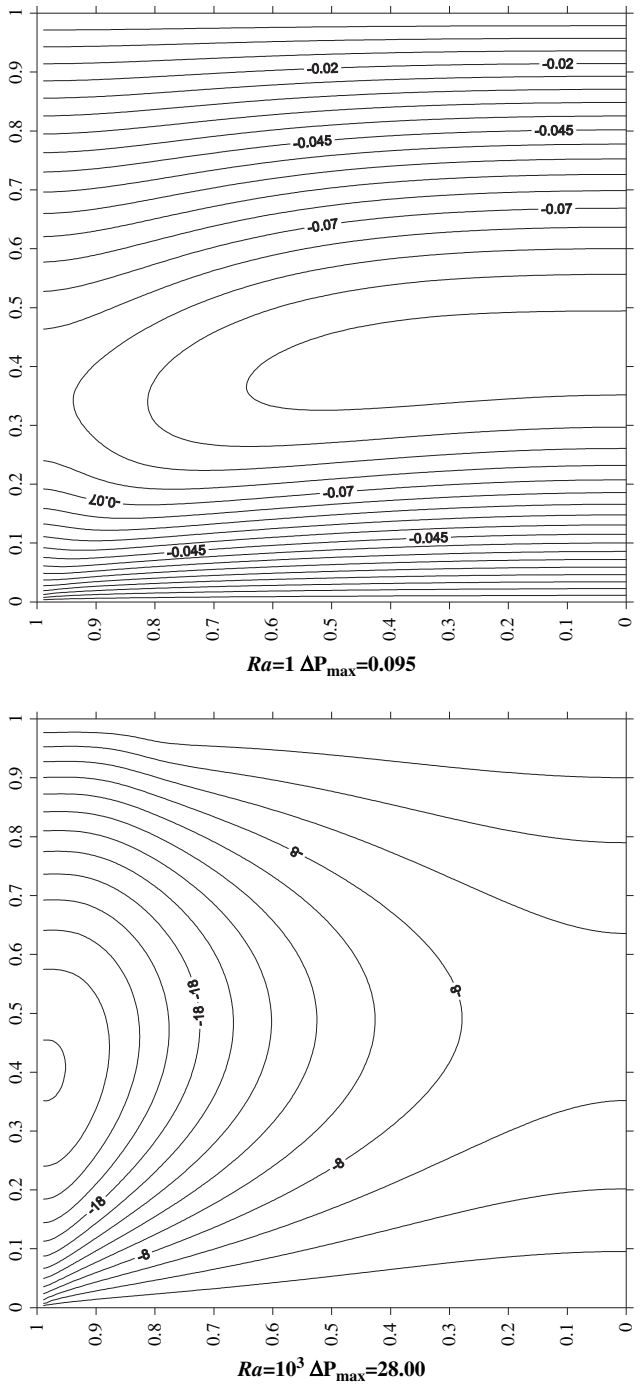

Fig. 6. Pressure distribution for different Rayleigh numbers ($Bi = 0.01$, $A = 1$, $XA = 0$).

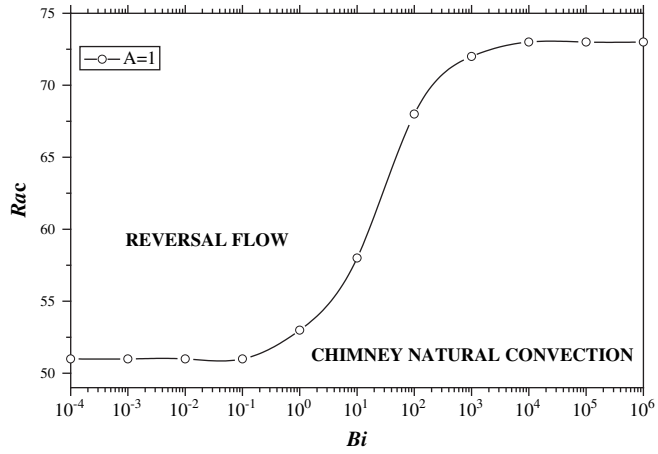

Fig. 7. Critical Rayleigh number versus the Biot number for $A = 1$ and $XA = 0$.

4.2. Sinusoidal wall temperature

To obtain an overall comparison of the heat transfer characteristics for the time-depending heating condition, the influences of the temperature oscillation on the relative heat transfer variation $((Nu_T - Nu)/Nu)$ are presented in Fig. 11 for different Rayleigh numbers, amplitudes and a low Biot number ($Bi = 0.01$).

First, the space averaged Nusselt number (Nu_m), for steady constant wall temperature ($XA = 0$) is shown in Fig. 8 versus Rayleigh and Biot numbers. This plot clearly indicates the increase of heat transfer with Rayleigh number. The flow enhancement with buoyancy forces increases the thermal gradients near the lateral heated wall.

For low Rayleigh values, the heat transfer exhibits an asymptotic value corresponding to the diffusive regime. The obtained conductive (low *Ra*) values are *Bi* dependent. The analytical conductive heat transfer coefficients (Eq. (22)) are plotted (Fig. 8) for different values of *Bi*. A good agreement is observed between the analytical and the numerical results.

It is observed that the heat transfer increases with the Biot number only for low Rayleigh number values. This is not the case for high Rayleigh numbers for which the flow exhibits a boundary layer structure where the weight effect of the exit boundary condition on the global flow decreases. Consequently all the curves, for different Biot numbers, tend to the boundary layer convective heat transfer. The resulting heat transfer variation ($Nu \sim 1/\delta$) is given by

$$Nu \sim Ra^{1/2} \tag{23}$$

The Nusselt number in the boundary layer regime is represented by the dashed line in Fig. 8. The resulting fitted *Nu* curve is given by

$$Nu = 0.695 \times Ra^{0.49} \tag{24}$$

Note that Simpkins and Blythe [29] gave correlation for the case of heat transfer in a rectangular porous cavity fitted like: $Nu = 0.51 \times Ra^{0.51}$. This correlation is fitted on the same figure. The difference between the two cases is probably due to the cylindrical strangulation (effect of the radius) which growth the flow rate and then the heat transfer.

Fig. 9a and b illustrates the temporal evolution of the space averaged Nusselt for different Rayleigh numbers and different dimensionless amplitudes. The monitoring points (1, 2, 3, 4) correspond to the temporal position over the sinusoidal wall temperature (see Fig. 2).

Initially, all the curves illustrate a transition from the conductive regime to an oscillatory behaviour. An exponential damping of the heat transfer fluctuation is clearly observed. The time period

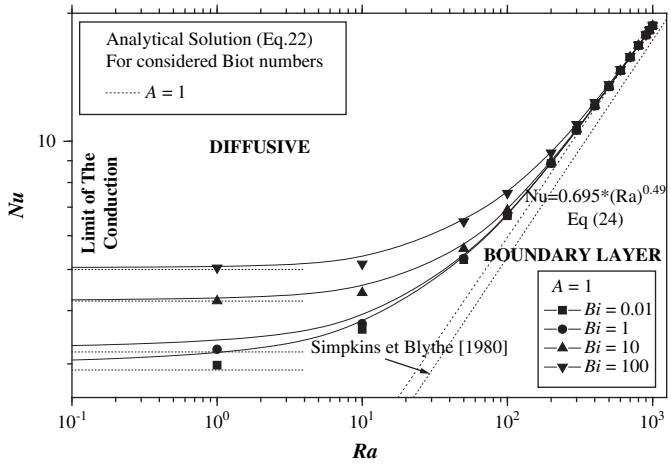

Fig. 8. The average Nusselt number (*Nu*) versus *Ra* for different *Bi*, for $A = 1$ and $XA = 0$.

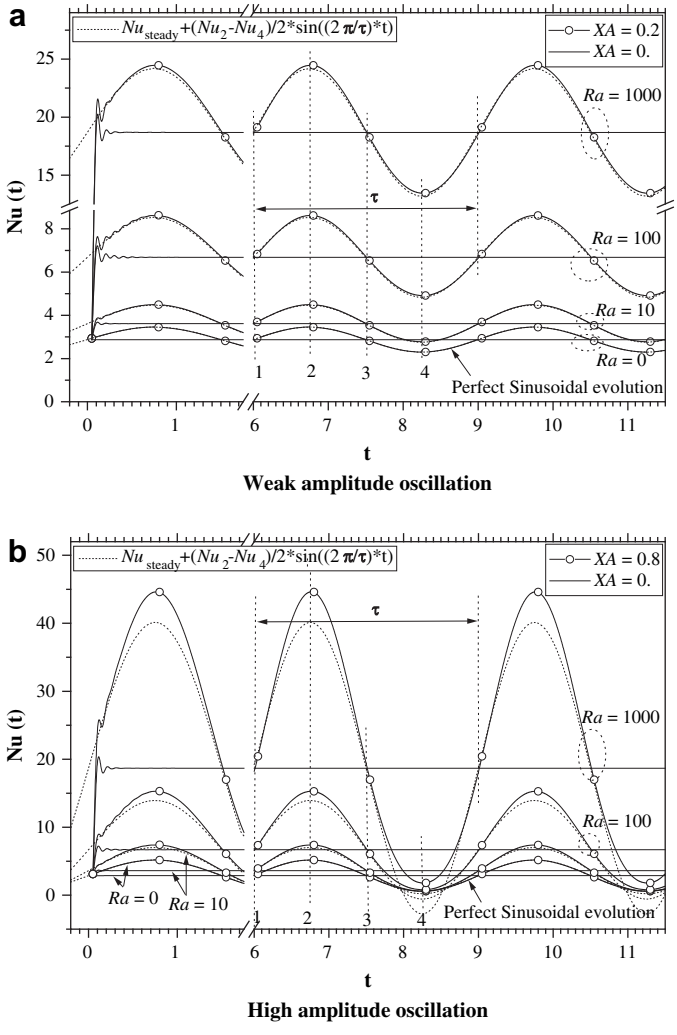

Fig. 9. The space averaged Nusselt number (Eq. (13)) evolution for different wall temperature oscillation amplitude, *XA* ($Ra = 100$, $A = 1$ and $Bi = 0.01$).

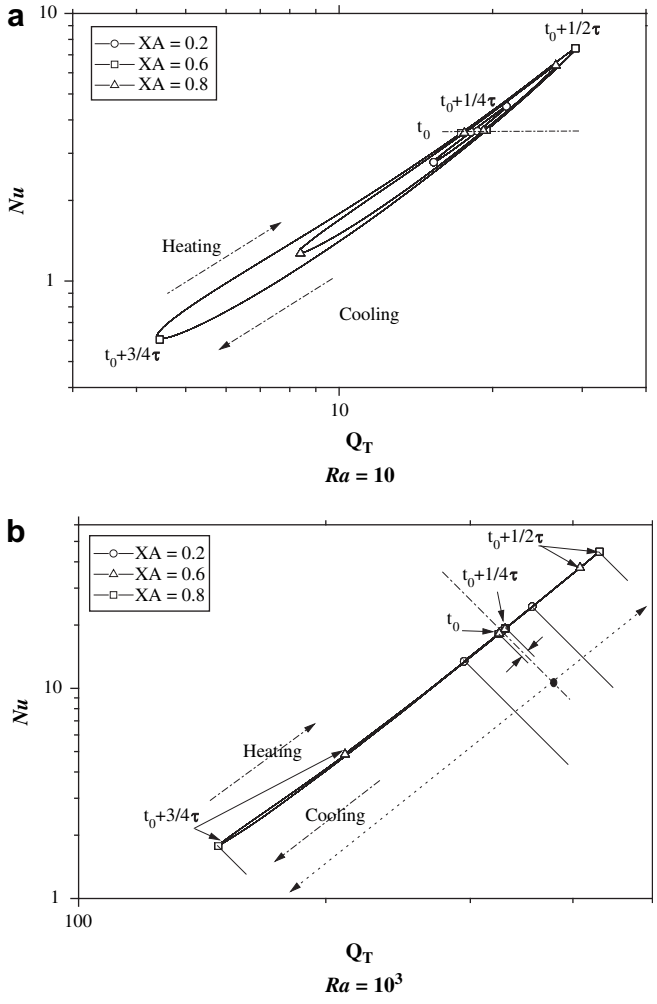

Fig. 10. Phase diagrams (Nu–Q_T) for different wall temperature oscillation amplitude, XA ($Bi = 0.01$ and $A = 1$).

required for these transitions decreases with the increase of the Rayleigh number. After the transition period the curves show a periodical evolution where the constant temperature formulation corresponds to the case of very low dimensionless amplitude ($XA \ll 1$).

For the presented tests, the temperature variation oscillation period is fixed as $\tau = 3$. In the conductive regime ($Ra = 0$), the temporal evolution of the heat transfer is mainly sinusoidal for all the considered amplitudes, and the Nu evolution can be predicted as

$$Nu = Nu_{\text{steady}} + ((Nu_2 - Nu_4)/2) \times \sin((2\pi/\tau) \times t) \qquad (25)$$

where Nu_{steady} is the obtained steady state Nusselt with constant temperature ($XA = 0$). Nu_2 and Nu_4 are respectively the Nusselt numbers at times noted 2 and 4, respectively.

The increase of Rayleigh number induces a loss of the symmetry time-evolution in comparison to the constant wall temperature case. This dissymmetry is more pronounced with the increase of the dimensionless amplitude (XA). In such non-symmetrical case Eq. (25) is not valid.

Fig. 10a and b shows the phase diagrams of heat transfer-flow rate (Nu–Q_T) for the two cases of low and high Rayleigh numbers, respectively. The closed loops clearly indicate the periodicity of the phenomena in these two situations. The phase shift and the Nu loss of symmetry exhibit an average time space Nusselt different from the steady state reference case.

For low Rayleigh numbers (Fig. 9a), it is observed that there is no phase shift in the response of the system (points 1 and 3 are on the same horizontal). Elsewhere for high Ra, the heat transfer is controlled by the aspirated fluid flow.

Fig. 11 illustrates the effect of the dimensionless amplitude on the relative heat transfer enhancement ($\Delta Nu/Nu$), for different Rayleigh values. For low dimensionless amplitudes ($XA < 0.5$), we observe an equivalence between constant and time-dependent heating conditions (relative change is less than 5%).

For amplitudes bigger than 0.5 we observe a significant heat transfer enhancement. These latter increases for high Rayleigh values. The heat transfer difference goes from the reference value (i.e. equivalence between constant and sinusoidal variation) to an increase of 19.5% while the dimensionless amplitude reaches 0.99.

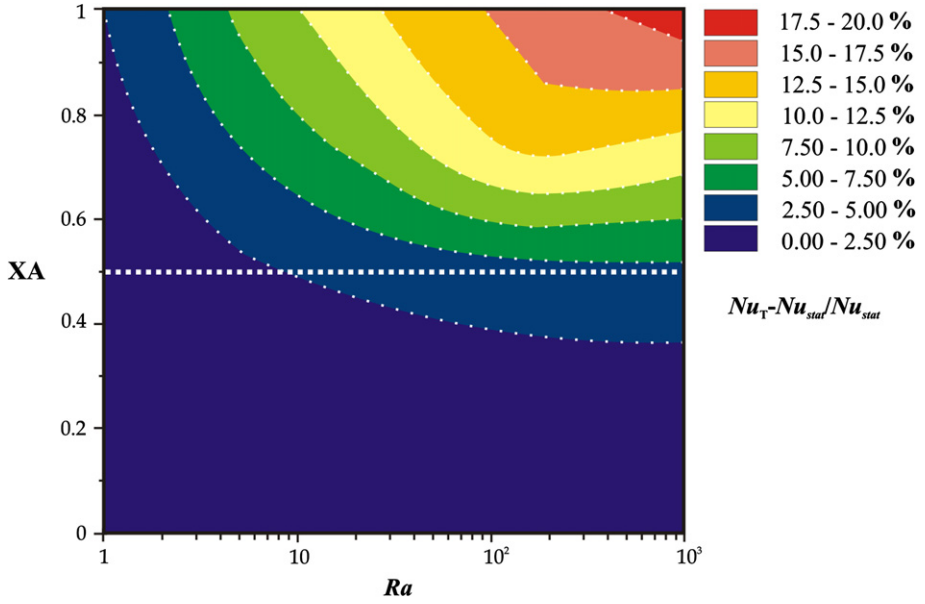

Fig. 11. Influence of the temperature oscillation on the relative heat transfer.

5. Conclusion

The problem of natural convection heat transfer in a vertical cylinder with open ends (which can be a vertical storage silo), filled with a fluid-saturated porous medium and heated with a sinusoidal lateral wall temperature, was the main focus of the present work. The results showed two types of flow, the main one is mainly unidirectional and the other one exhibits the presence of counter-flows.

The reverse flow function of *Ra* and *Bi* is a result of the pressure gradient effect occurring outside the thermal boundary layer.

The *Bi* effect illustrates three principal domains:

- The weak and high *Bi* values exhibit a constant asymptotic R_c tendency.
- The intermediate *Bi* values exhibit an increase of Ra_c with *Bi* connecting the two asymptotic values.

The periodical heating was analysed and gives important results.

For the low dimensionless amplitudes case ($XA < 0.5$), the resulting heat transfer in the sinusoidal time variation case is equivalent to the case of constant wall temperature with a difference less than 5%.

For high Rayleigh number, the resulting heat transfer from the sinusoidal time variation case and the constant wall temperature case is different, and the heat transfer difference increases up to 20% when the dimensionless amplitude reaches 0.99. This result gives the validity domain of the constant temperature formulation which is closely dependent with the temperature oscillation.

Acknowledgments

The author would like to express his thanks to Prof. P. Vasseur (Ecole Polytechnique de Montreal) and Prof. A.A. Mohamad (Calgary University) for the correction and the fruitfull discussion.

References

[1] J.C. Patterson, J. Imberger, Unsteady natural convection in a rectangular cavity, Int. J. Fluid Mech. 100 (1980) 65–86.
[2] J.D. Hall, A. Bejan, J.B. Chaddock, Transient natural convection in a rectangular enclosure with one heated side wall, Int. J. Heat Fluid Flow 9 (1988) 396–404.
[3] P. Vasseur, L. Robillard, Natural convection in a rectangular cavity with wall temperature decreasing at uniform misses, Warme-und Stoffubertragung 16 (1982) 199–207.
[4] M. Kazmierczak, Z. Chinoda, Boundary-driven flow in an enclosure with time periodic boundary conditions, Int. J. Heat Mass Transfer 35 (1992) 1507–1518.
[5] W.J. Mantle-Miller, M. Kazmierczak, B. Hiawy, Natural convection in a horizontal enclosure with periodically changing bottom wall temperature, in: ASME 28th National Heat Transfer Conference, 1992, HTD-198, pp. 49–56.
[6] M. Sözen, K. Vafai, Analysis of oscillating compressible flow through a packed bed, Int. J. Heat Fluid Flow 12 (1991) 130–136.
[7] R. Bradean, D.B. Ingham, P.J. Heggs, I. Pop, Free convection fluid flow due to a periodically heated and cooled vertical plate embedded in a porous media, Int. J. Heat Mass Transfer 39 (1995) 2545–2557.
[8] R. Bradean, D.B. Ingham, P.J. Heggs, I. Pop, Unsteady free convection adjacent to an impulsively heated horizontal circular in porous media, Num. Heat Transfer-A 32 (1997) 325–346.
[9] B.V. Antohe, J.L. Lage, Amplitude effect on convection induced by time-periodic heating, Int. J. Heat Mass Transfer 39 (1996) 1121–1133.
[10] G. Desrayaud, R. Bennacer, J.P. Caltagirone, É. Chenier, A. Joulin, N. Laaroussi, K. Mojtabi, Étude numérique comparative des écoulements thermoconvectifs dans un canal vertical chauffé asymétriquement, VIIIème Colloque Interuniversitaire Franco-Québécois, Montréal, Canada, 28–30 mai 2007.
[11] A.S. Krishnan, B. Premachandran, C. Balaji, S.P. Venkateshan, Combined experimental and numerical approaches to multi-mode heat transfer between vertical parallel plates, Exp. Therm. Fluid Sci. 29 (2004) 75–86.
[12] J. Hernandez, B. Zamora, Effects of variable properties and non-uniform heating on natural convection flows in vertical channels, Int. J. Heat Mass Transfer 48 (2005) 793–807.
[13] J. Boland, The analytic solution of the differential equations describing heat flow in houses, Build. Environ. 37 (2002) 1027–1035.
[14] S.V. Patankar, Numerical Heat Transfer Fluid Flux, Hemisphere/McGraw-Hill, New York, 1980.
[15] R. Bennacer, M. El Ganaoui, E. Leonardi, Vertical Bridgman configuration heated from below: 3D bifurcation and stability analysis, Appl. Math. Model. 30 (11) (2006) 1249–1261.
[16] D.E. Ameziani, K. Bouhadef, R. Bennacer, O. Rahli, Analysis of the chimney natural convection in a vertical porous cylinder, Numer. Heat Transfer A 54 (2008) 47–66.
[17] K.L. Walker, G.M. Homsy, Convection in a porous cavity, J. Fluid Mech. 87 (1978) 449–474.
[18] O.V. Trevisan, A. Bejan, Natural convection with combined heat mass transfer buoyancy effects in a porous medium, Int. J. Heat Mass Transfer 28 (1985) 1597–1611.
[19] G. Lauriat, V. Prasad, Non-Darcian effect on natural convection in a vertical porous enclosure, Int. J. Heat Mass Transfer 32 (1989) 2135–2148.
[20] P. Nithiarasu, K.N. Seetaramu, T. Sundarajan, Natural convective heat transfer in an enclosure filled with a fluid saturated variable porosity medium, Int. J. Heat Mass Transfer 40 (1997) 3955–3967.
[21] P. Nithiarasu, K.N. Seetaramu, T. Sundarajan, Non-Darcy double-diffusive convection in a fluid saturated axisymetric porous cavities, Heat Mass Transfer 36 (1997) 427–434.
[22] P. Nithiarasu, K.N. Seetaramu, T. Sundarajan, Double-diffusive convection in a fluid saturated axisymetric porous cavity with freely convecting wall, Int. Comm. Heat Mass Transfer 24 (1997) 1121–1130.
[23] P. Nithiarasu, K. Ravindran, A new semi-implicit time stepping procedure for buoyancy driven flow in a fluid saturated porous medium, Comput. Methods Appl. Mech. Eng. 165 (1998) 147–154.
[24] A.C. Baytas, Entropy generation for natural convection in an inclined porous cavity, Int. J. Heat Mass Transfer 43 (2000) 2089–2099.
[25] N. Massarotti, P. Nithiarasu, O.C. Zienkiewicz, Natural convection in porous medium–fluid interface problems. A finite element analysis by using the CBS procedure, Int. J. Num. Methods Heat fluid flow 11 (5) (2001) 473–490.
[26] R. Bennacer, A. Tobbal, H. Beji, P. Vasseur, Double diffusive convection in a vertical enclosure filled with anisotropic porous media, Int. J. Therm. Sci. 40 (2001) 30–41.
[27] N.H. Saeid, I. Pop, Non-Darcy natural convection in a square cavity filled with a porous medium, Fluid Dyn. Res. 36 (2005) 35–43.
[28] S. Benasrallah, T. Amara, M.A. Du Peuty, Convection naturelle instationnaire dans un cylindre rempli de grains ouvert à ses extrémités et dont la paroi est chauffée par un flux de chaleur constant: validité de l'hypothèse de l'équilibre thermique local, Int. J. Heat Mass Transfer 40 (1997) 1115–1168.
[29] G. Simpkins, P.A. Blythe, Convection in porous layer, Int. J. Heat Mass Transfer 23 (1980) 881–887.